An ozone increase in the Antarctic summer stratosphere: A dynamical response to the ozone hole

R. S. Stolarski,[1] A. R. Douglass,[1] M. Gupta,[1,2] P. A. Newman,[1] S. Pawson,[3] M. R. Schoeberl,[4] and J. E. Nielsen[5]

[1] Profiles of ozone concentration retrieved from the SBUV series of satellites show an increase between 1979 and 1997 in the summertime Antarctic middle stratosphere ($\sim$25–10 hPa). Data over the South Pole from ozone sondes confirm the increase. A similar ozone increase is produced in a chemistry climate model that allows feedback between constituent changes and the stratospheric circulation through radiative heating. A simulation that excludes the radiative coupling between predicted ozone and the circulation does not capture this ozone increase. We show that the ozone increase in our model simulations is caused by a dynamical feedback in response to the changes in the stratospheric wind fields forced by the radiative perturbation associated with the Antarctic ozone hole. **Citation:** Stolarski, R. S., A. R. Douglass, M. Gupta, P. A. Newman, S. Pawson, M. R. Schoeberl, and J. E. Nielsen (2006), An ozone increase in the Antarctic summer stratosphere: A dynamical response to the ozone hole, *Geophys. Res. Lett.*, *33*, L21805, doi:10.1029/2006GL026820.

1. Introduction

[2] The ozone loss leading to the Antarctic ozone hole has been observed to occur during springtime, in the lower stratosphere, between altitudes of about 12 and 22 kilometers ($\sim$150–25 hPa) [*Hofmann et al.*, 1997]. This paper examines the seasonal variation of ozone trends in the 25–10 hPa layer using data from the Solar Backscatter Ultraviolet (SBUV) series of instruments and from ozone sondes launched from the South Pole station. Time series analysis of this data indicates small negative trends in ozone concentration, except during the summer months when trends are positive.

[3] Chemistry/transport models (CTMs) reproduce many observed behaviors of stratospheric ozone and other minor constituents [e.g., *Douglass et al.*, 2004; *Stolarski et al.*, 2006]. CTMs do not have the feedback processes between trace gases and the radiation field that provide a mechanism for changes in trace gases to affect the circulation of the stratosphere and modify the trace-gas response to forcing. The importance of these feedbacks can be estimated with a model that allows interactions among its radiative, chemical, and dynamical components. Chemistry/climate models (CCMs) combine a general circulation model (GCM) with a representation of photochemistry developed for CTMs [e.g. *Austin et al.*, 2003; *Eyring et al.*, 2006]. We combined the GEOS-4 GCM (Goddard Earth Observing System, Version 4, General Circulation Model) with the photochemistry from our stratospheric CTM to produce the GEOS CCM.

[4] Prior studies have examined changes associated with the Antarctic ozone hole, but have neither focused on the region of ozone increase that overlies the region of depletion nor isolated the signature of ozone increase in observations. The ozone increase is surprising and is not a direct effect of the increase in chlorine or bromine, which are expected to increase the loss of ozone throughout the stratosphere. Several CCMs have calculated a warmer layer in the Antarctic spring above the cooled region of the ozone hole [e.g., *Kiehl et al.*, 1988; *Mahlman et al.*, 1994]. Similar ozone changes to those reported here are evident in prior CCM studies [e.g., *Austin*, 2002; *Langematz et al.*, 2003; *Manzini et al.*, 2003] but the cause of the increase has not been discussed in detail.

[5] In the following section we describe the ozone increase as seen in ground- and space-based observations. The GEOS CCM and the simulations used here are described in Section 3, and are used to explain the formation and generation of the observed ozone enhancement in Section 4.

2. Observed Trends in the Antarctic Summer Ozone Profile

[6] A series of SBUV instruments yields stratospheric ozone profiles between 50 and 1 hPa. The Version 8 (V8) processing algorithm derives profiles with information on vertical scales of about 5 km [*Bhartia et al.*, 1996; *DeLand et al.*, 2004; *Bhartia et al.*, 2004; *Taylor et al.*, 2003]. The V8 processing algorithm homogenizes the data record through re-calibration of each SBUV instrument. Use of a time-independent *a priori* in the retrievals and the calibration of each SBUV instrument to the same scale prevents artificial trends in the data set.

[7] Following *Stolarski et al.* [2006], statistical analysis of the time series of SBUV retrievals between 1979 and 2003 was performed for months that are sunlit at high southern latitudes (October–April). Explanatory variables in the statistical model include seasonal cycle, equivalent effective stratospheric chlorine (EESC), the quasi-biennial oscillation, volcanic aerosols and the solar cycle. The ozone trend for 1979–1997 is the projection on to EESC term, which increases linearly in this period, before leveling off.

[1]Atmospheric Chemistry and Dynamics Branch, NASA Goddard Space Flight Center, Greenbelt, Maryland, USA.
[2]Office of Environment and Energy, Federal Aviation Administration, Washington, DC, USA.
[3]Global Modeling and Assimilation Office, NASA Goddard Space Flight Center, Greenbelt, Maryland, USA.
[4]Earth Science Directorate, NASA Goddard Space Flight Center, Greenbelt, Maryland, USA.
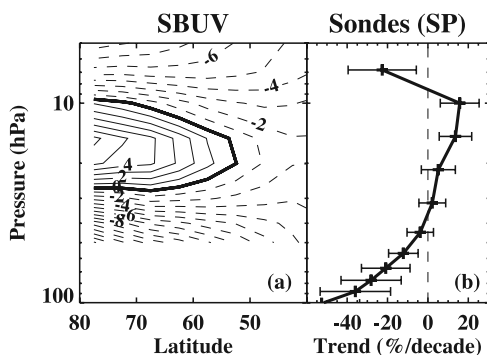[5]Science Systems and Applications, Inc., Lanham, Maryland, USA.

Figure 1. (a) Latitude-pressure cross-section of the zonal mean ozone trend due to change in EESC for 1979–1997 determined from SBUV data for December. Units are percent per decade, with a contour spacing of 1%/decade. Trends greater than about 5%/decade are significant at the 2σ level. (b) December ozone trend determined from South Pole ozonesondes using data from 1962–1987. The error bars represent 2σ statistical uncertainty in the trend.

Figure 1a shows the latitude-pressure cross-section of the linear 1979–1997 ozone trend for December. The negative trend in the lower stratosphere is the remnant of the ozone hole. Above this, ozone increases in the 25–10 hPa layer between 80°S and nearly 50°S. The positive trend reaches 6% per decade at 15 hPa and 75–80°S. The ozone column within this positive layer is about 50 DU out of a total column of about 300 DU observed during December. The positive trend in the 25–10 hPa layer between 75°S and 80°S is a little larger than 2 DU/decade, while the trend in the total column in the same latitude band is −30 DU/decade. Thus the positive region compensates slightly for the large negative trend due to the photochemical processes that cause the ozone hole.

[8] South Pole ozone sonde profiles for 1962–2005 were also analyzed. Figure 1b shows that the ozone trend due to change in EESC deduced from the ozonesonde observations for December is comparable with that determined from SBUV data. The maximum positive trend is $15 \pm 8\%$ (2σ) per decade near 10 hPa. The maximum trend is only 10%/decade when averaged over the SBUV weighting function, making it comparable to the SBUV observations within uncertainties. The uncertainties are larger for the trends from the ozonesonde profiles than those from the SBUV ($\sim\pm5\%$/decade) because each profile represents a single point and there are gaps in the record.

[9] The SBUV instruments make measurements up to 80°S during the sunlit summer months. Figure 2 shows the trends calculated from the SBUV data between 5 and 50 hPa as a function of month. The positive trend region first appears at about 10 hPa during October. The peak of the positive trend region appears at progressively lower altitudes until it disappears in February.

3. Model Simulations

[10] We use simulations from our CTM and the GEOS CCM to investigate the role of dynamic feedback in producing the observed changes in summertime Antarctic ozone. *Stolarski et al.* [2006] describe the CTM simulation.

It was driven by meteorological fields from a 50-year integration of the GEOS-4 GCM. This integration of the GCM used a fixed ozone climatology in its radiation code. That climatology was consistent with the mid 1990s including an ozone hole. With fixed composition of radiatively active gases there were no radiatively-induced changes in climate. The CTM's stratospheric photochemistry includes the known important reactions [*Sander et al.*, 2003]. The 50-year simulation used time-dependent mixing ratios of CFCs and other source gases specified at the lower boundary following World Meteorological Organization (WMO) scenario A2 [*WMO*, 2003]. Trends in ozone as a function of latitude, altitude, and season were presented by *Stolarski et al.* [2006].

[11] The GEOS CCM couples the GEOS-4 GCM [*Bloom et al.*, 2005] with the stratospheric chemistry module from the CTM. The simulated concentrations of CO_2 H_2O, N_2O, O_3, CH_4, CFC-11, and CFC-12 used to determine heating and cooling rates. Two "time-slice" simulations of the GEOS CCM are used to investigate the cause of the change in ozone profile. Each simulation was run for 25 years using sea-surface temperature and sea-ice boundary conditions for the period 1979–2004 [*Rayner et al.*, 2003]. This ensures that all differences in the simulations are explained by internal processes and the external physical forcing mechanisms are unchanged. Trace gas boundary conditions were specified for 1975 in the "1980" simulation and 1995 in the "2000" simulation. This five-year lag approximately accounts for transport times through the system, so that radiatively active and ozone-depleting gases reach appropriate values for the years of interest.

[12] Figure 3 compares the ozone trends in the Antarctic summer from the coupled GEOS CCM simulations with trends calculated from time-series analysis of the simulation with the uncoupled CTM. The GEOS CCM trends are the difference of the two time-slice simulations in percent per decade. The CCM shows a feature similar to that seen in the SBUV data (Figure 2). The CTM trend in that region is small, but there is no significant positive response. The positive response of ozone in the coupled GEOS CCM simulation is about 50% larger than observed and the
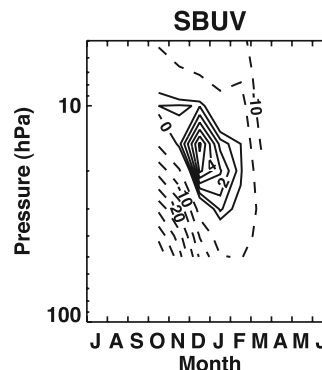

Figure 2. Trends calculated from SBUV data for the latitude band between 75°S and 80°S as a function of month of the year. Data is available for trend calculation only for the summer months when the polar region is sunlit. Positive contours are spaced by 1%/decade while negative contours are every 5%/decade.
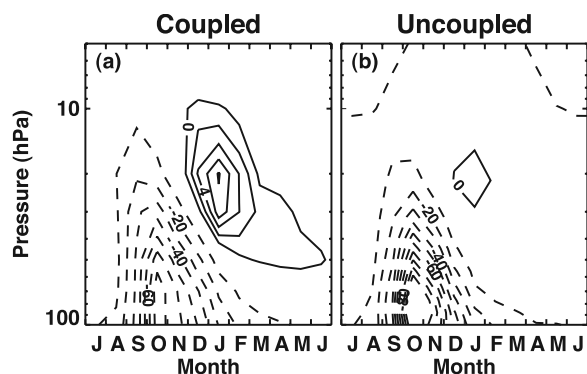
Figure 3. (a) Ozone trend from the GEOS CCM and (b) ozone trend from the CTM as a function of month and altitude. Positive contours are spaced by 2%/decade. Negative contours are spaced by 5%/decade.

maximum is displaced in time by 2–3 weeks. This offset is consistent with the late breakup of the Antarctic polar vortex in the GEOS CCM.

4. Feedback Mechanism Causing Ozone Increase

[13] Unlike the uncoupled CTM simulation, the GEOS CCM simulations produce a positive ozone trend similar to that derived from observations, suggesting that feedback processes provide the explanation for the ozone increase. The dynamical response to increased greenhouse gases and chlorine/bromine loading in the GEOS CCM is broadly similar to that in several prior studies. *Langematz et al.* [2003] imposed ozone and CO_2 changes in a GCM and found that the breakdown of the Antarctic polar vortex was delayed, in broad agreement with observations [e.g. *Randel and Wu*, 1999; *Waugh et al.*, 1999]. Temperature changes included cooling of the low stratosphere into November and December, with a warmer layer above. Similar changes are seen in the GEOS CCM. The ozone-hole induced cooling of the low stratosphere in the polar region leads to a delay

in the downward propagation of the vortex breakdown. *Langematz et al.* [2003] also showed increased descent in the residual circulation over Antarctica in the December–January–February average, which is reproduced in the present model. Other CCM simulations [*Austin*, 2002; *Manzini et al.*, 2003] show some ozone increase above the ozone-hole, but no substantive explanations have been given.

[14] An explanation of the positive trends is now given. Time series of December averaged ozone concentrations at 20 hPa display both a positive trend and year-to-year fluctuations (not shown). The polar ozone fluctuations for December are correlated with the strength of the zonal jet (Figure 4, left), with a stronger polar vortex in the lower stratosphere (50 hPa and 60°S) corresponding to a larger polar ozone anomaly near 20 hPa. This relationship clearly shows that the ozone trend has the same mechanism as the interannual variability, with a preferred tendency of late vortex breakdowns in the 1990s compared to the 1980s. Interannual variability in the 1980 and 2000 time-slice simulations is very similar to that in the real atmosphere (Figure 4, right), despite the tendency of the Antarctic polar vortex to break down too late. The late vortex breakdown in the simulations results in a larger range of values in the CCM than in the real atmosphere, but the relationship between anomalies in the vortex and the ozone is well represented in the model. Further, the GEOS CCM shows a similar tendency as the observations, in that the vortex tends to break down later under 2000 chlorine loading (open squares) than under 1980 conditions (solid squares).

[15] The analysis has so far demonstrated that the simulated vortex breaks down later under 2000 conditions, as in the real atmosphere, and that the relationship between the polar vortex and the 20-hPa polar ozone anomaly is captured. It remains to demonstrate the cause of the ozone anomaly. As in the work of *Langematz et al.* [2003], the persistent polar vortex allows for vertical propagation of planetary waves; as these dissipate near the shear zone they induce descent in the residual circulation. In the 1980 simulation there is weak upwelling above 10 hPa and
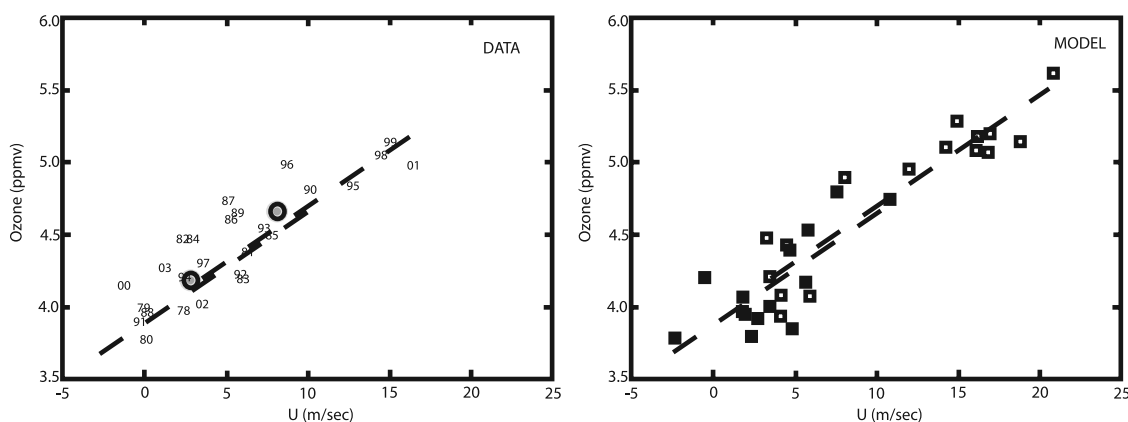

Figure 4. Relationship between ozone concentration in positive region (20 hPa, 75–80S) and zonal wind near vortex edge (50 hPa, 60S) for December. (left) SBUV data and NCEP analyses with each point indicated by the year. The filled circles are the average for the first 6 years (1978–1983) and for the last 6 years (1998–2003). The dashed lines are the linear fit to the model results shown in Figure 4 (right). (right) Results from the CCM simulation. Filled squares are the 1980 time-slice simulation and open squares are the 2000 simulation. The circles indicate the average of each simulation and the dashed lines are a linear fit to each of the simulations.
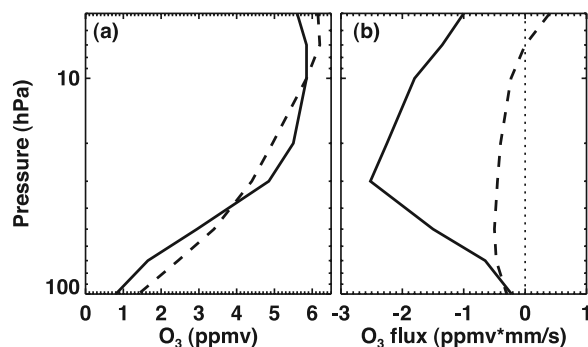
Figure 5. Profiles of (a) ozone and (b) mean vertical ozone flux averaged over the polar cap (60−90S) for 1980 (dashed lines) and 2000 (solid lines). Each curve shows the average of data from 20 representations of January 1 from the two time-slice simulations of the GEOS CCM.

weak downwelling below 10 hPa, but in the 2000 simulation the persistence of the vortex leads to a downwelling (typically 3 mm/s averaged over the polar cap) at all layers. The result of this can be seen in Figure 5, which shows the polar-mean ozone profile and the vertical transport, averaged over the polar cap (60−90°S) on January 1 in the 1980 and 2000 simulations. The 30−10 hPa ozone increase in 2000 is evident, with reduced concentrations in the remnants of the polar vortex and above 10 hPa. There is a large change in downward ozone transport (computed as the product of the ozone concentration and the residual vertical velocity) that arises mainly because of the increased downwelling in the polar region. This is the cause of the ozone change (Figure 3a) and the correlation between ozone increase near 20 hPa and the polar vortex breakdown (Figure 4, right).

5. Discussion and Conclusion

[16] We have found a region of the middle stratosphere in the Antarctic summer where ozone increased between 1980 and 2000. This region of increase is seen in the data from the SBUV series of satellites and is confirmed by ozone-sondes launched over the South Pole station.

[17] We have explained the increase as a dynamical feedback where ozone is increased in a way that can interpreted as a "dynamical self-healing". Specifically, the delay in vortex breakdown induced by the ozone hole establishes a perturbed transport, with stronger descent of ozone-rich air into the polar cap near 20 hPa. As the ozone hole recovers in the future with the removal of stratospheric chlorine and bromine, we expect that this ozone anomaly will disappear unless the polar vortex breakdown is substantially delayed by further increases in greenhouse gases.

References

Austin, J. (2002), A three-dimensional coupled chemistry-climate model simulation of past stratospheric trends, *J. Atmos. Sci.*, *59*, 218−232.

Austin, J., et al. (2003), Uncertainties and assessments of chemistry-climate models of the stratosphere, *Atmos. Chem. Phys.*, *3*, 1−27.

Bhartia, P. K., R. D. McPeters, C. L. Mateer, L. E. Flynn, and C. Wellemeyer (1996), Algorithm for the estimation of vertical ozone profiles from the backscattered ultraviolet technique, *J. Geophys. Res.*, *101*, 18,793−18,806.

Bhartia, P. K., R. D. McPeters, R. S. Stolarski, L. E. Flynn, and C. G. Wellemeyer (2004), A quarter century of ozone observations by SBUV and TOMS, paper presented at XX Quadrennial Ozone Symposium, Int. Ozone Comm., Kos, Greece, 1−8 June.

Bloom, S., et al. (2005), The Goddard Earth Observation System Data Assimilation System, GEOS DAS version 4.0.3: Documentation and validation, *NASA Tech. Memo., TM-2005-104606*, vol. 26, 166 pp.

DeLand, M. T., L.-K. Huang, S. L. Taylor, C. A. McKay, R. P. Cebula, P. K. Bhartia, and R. D. McPeters (2004), Long-term SBUV and SBUV/2 instrument calibration for version 8 data, paper presented at XX Quadrennial Ozone Symposium, Int. Ozone Comm., Kos, Greece, 1−8 June.

Douglass, A. R., R. S. Stolarski, S. E. Strahan, and P. S. Connell (2004), Radicals and reservoirs in the GMI chemistry and transport model: Comparison to measurements, *J. Geophys. Res.*, *109*, D16302, doi:10.1029/2004JD004632.

Eyring, V., et al. (2006), Assessment of temperature, trace species, and ozone in chemistry-climate model simulations of the recent past, *J. Geophys. Res.*, doi:10.1029/2006JD007327, in press.

Hofmann, D. J., S. J. Oltmans, J. M. Harris, B. J. Johnson, and J. A. Lathrop (1997), Ten years of ozonesonde measurements at the south pole: Implications for recovery of springtime Antarctic ozone, *J. Geophys. Res.*, *102*, 8931−8943.

Kiehl, J. T., B. A. Boville, and B. P. Briegleb (1988), Response of a general circulation model to a prescribed Antarctic ozone hole, *Nature*, *332*, 501−504.

Langematz, U., M. Kunze, K. Kruger, K. Labitzke, and G. L. Roff (2003), Thermal and dynamical changes of the stratosphere since 1979 and their link to ozone and CO_2 changes, *J. Geophys. Res.*, *108*(D1), 4027, doi:10.1029/2002JD002069.

Mahlman, J. D., J. P. Pinto, and L. J. Umscheid (1994), Transport, radiative, and dynamical effects of the Antarctic ozone hole: A GFDL "SYYHI" model experiment, *J. Atmos. Sci.*, *51*, 489−508.

Manzini, E., B. Steil, C. Brühl, M. A. Giorgetta, and K. Krüger (2003), A new interactive chemistry climate model: 2. Sensitivity of the middle atmosphere to ozone depletion and increase in greenhouse gases and implications for recent stratospheric cooling, *J. Geophys. Res.*, *108*(D14), 4429, doi:10.1029/2002JD002977.

Randel, W. F., and F. Wu (1999), A stratospheric ozone trends data set for global modeling studies, *Geophys. Res. Lett.*, *26*, 3089−3092.

Rayner, N. A., D. E. Parker, E. B. Horton, C. K. Folland, L. V. Alexander, D. P. Rowell, E. C. Kent, and A. Kaplan (2003), Global analyses of sea surface temperature, sea ice, and night marine air temperature since the late nineteenth century, *J. Geophys. Res.*, *108*(D14), 4407, doi:10.1029/2002JD002670.

Sander, S. P., et al. (Eds.) (2003), Chemical kinetics and photochemical data for use in atmospheric studies, *JPL Publ., 02-25*.

Stolarski, R. S., A. R. Douglass, S. Steenrod, and S. Pawson (2006), Trends in stratospheric ozone: Lessons learned from a 3D chemistry transport model, *J. Atmos. Sci.*, *63*, 1028−1041.

Taylor, S. L., R. P. Cebula, M. T. DeLand, L. K. Huang, R. S. Stolarski, and R. D. McPeters (2003), Improved calibration of NOAA-9 and NOAA-11 SBUV/2 total ozone data using in-flight validation methods, *Int. J. Remote Sens.*, *24*, 315−328.

Waugh, D. W., W. J. Randel, S. Pawson, P. A. Newman, and E. R. Nash (1999), Persistence of the lower stratospheric vortices, *J. Geophys. Res.*, *104*, 27,191−27,201.

World Meteorological Organization (2003), Scientific assessment of ozone depletion: 2002, *Global Ozone Res. Monit. Proj. Rep. 47*, Geneva, Switzerland.

————————————

A. R. Douglass, M. Gupta, P. A. Newman, and R. S. Stolarski, Atmospheric Chemistry and Dynamics Branch, NASA Goddard Space Flight Center, Code 613.3, Greenbelt, MD 20771, USA. (richard.s.stolarski@nasa. gov)

J. E. Nielsen, Science Systems and Applications, Inc., 10210 Greenbelt Road, Lanham, MD 20706, USA.

S. Pawson, Global Modeling and Assimilation Office, NASA Goddard Space Flight Center, Code 610.1, Greenbelt, MD 20771, USA.

M. R. Schoeberl, Earth Science Directorate, NASA Goddard Space Flight Center, Code 613.3, Greenbelt, MD 20771, USA.